Effect of the N-Terminal Glycine on the Secondary Structure, Orientation, and Interaction of the Influenza Hemagglutinin Fusion Peptide with Lipid Bilayers

Cameron Gray,* Suren A. Tatulian,* Steve A. Wharton,‡ and Lukas K. Tamm*
*Department of Molecular Physiology and Biological Physics, University of Virginia School of Medicine, Charlottesville, Virginia 22908 USA, and ‡Division of Virology, MRC National Institute for Medical Research, Mill Hill, London NW7 1AA England

ABSTRACT The amino-terminal segment of the membrane-anchored subunit of influenza hemagglutinin (HA) plays a crucial role in membrane fusion and, hence, has been termed the fusion peptide. We have studied the secondary structure, orientation, and effects on the bilayer structure of synthetic peptides corresponding to the wild-type and several fusogenic and nonfusogenic mutants with altered N-termini of the influenza HA fusion peptide by fluorescence, circular dichroism, and Fourier transform infrared spectroscopy. All peptides contained segments of α-helical and β-strand conformation. In the wild-type fusion peptide, ~40% of all residues were in α-secondary and ~30% in β-secondary structures. By comparison, the nonfusogenic peptides exhibited larger β/α secondary structure ratios. The order parameters of the helices and the amide carbonyl groups of the β-strands of the wild-type fusion peptide were measured seperately, based on the infrared dichroism of the respective absorption bands. Order parameters in the range 0.1–0.7 were found for both segments of the wild-type peptide, which indicates that they are most likely aligned at oblique angles to the membrane normal. The nonfusogenic but not the fusogenic peptides induced splitting of the infrared absorption band at ~1735 cm^{-1}, which is assigned to stretching vibrations of the lipid ester carbonyl bond. This splitting, which reports on an alteration of the hydrogen bonds formed between the lipid ester carbonyls and water and/or hydrogen-donating groups of the fusion peptides, correlated with the β/α ratio of the peptides, suggesting that unpaired β-strands may replace water molecules and hydrogen-bond to the lipid ester carbonyl groups. The profound structural changes induced by single amino acid replacements at the extreme N-terminus of the fusion peptide further suggest that tertiary or quaternary structural interactions may be important when fusion peptides bind to lipid bilayers.

INTRODUCTION

Enveloped viruses enter cells by membrane fusion, which is mediated by spike glycoproteins of the viral envelope. Many fusion proteins, including the viral spike glycoproteins, contain a highly conserved, moderately hydrophobic sequence of about 20 to 25 residues called the fusion peptide, which inserts into the lipid bilayer of the target membrane during membrane fusion (Wiley and Skehel, 1987; Stegmann et al., 1987; White, 1990, 1992). The best characterized viral fusion protein is influenza hemagglutinin (HA). Influenza HA is activated by a protease, which cleaves the single polypeptide chain of the precursor (HA0) into two disulfide-linked polypeptides, HA1 and HA2. This proteolytic step liberates the fusion peptide, which is located at the newly formed N-terminus of the smaller, membrane-spanning polypeptide HA2. At neutral pH, the fusion peptide is buried in the stem region of the HA (Wilson et al., 1981) and is inaccessible to antibodies or membranes. When fusion is triggered by a drop of the pH inside the endosome below a critical threshold of 5.0 to 6.0, a large conformational change of HA occurs (Skehel et al., 1982; Carr and Kim, 1993; Bullough et al., 1994; Tatulian et al., 1995a), rendering the ectodomain (domain projecting outward from the viral membrane) amphiphilic, as demonstrated by its ability to bind to lipid bilayers (Skehel et al., 1982; Doms et al., 1985). The acquisition of amphiphilicity is mediated by the fusion peptide, which can insert into target (Harter et al., 1989; Stegmann et al., 1991; Tsurudome et al., 1992; Wharton et al., 1995) and viral (Weber et al., 1994; Wharton et al., 1995) membranes. The importance of the fusion peptide in HA-mediated membrane fusion is further confirmed by various lines of evidence: several point mutations introduced into the fusion peptide by site-directed mutagenesis either abolished or shifted the pH response of fusion (Gething et al., 1986), drugs that prevent the extrusion of the fusion peptide from its pH 7 location inhibited fusion (Bodian et al., 1993) and removal of the fusion peptide from otherwise intact HA by thermolysin digestion blocked membrane fusion (Ruigrok et al., 1988).

Several groups have studied lipid interactions and structural properties of synthetic fusion peptides corresponding to the N-terminus of wild-type influenza HA2. Lear and DeGrado (1987) showed that fusion peptides of HA of different lengths contained different proportions of helix, and that low pH induced increased helicity and a blue shift of the tryptophan fluorescence emission maximum. Murata et al. (1987, 1992) showed that a HA fusion peptide of a slightly different sequence promoted membrane fusion be-

Received for publication 16 November 1995 and in final form 7 February 1996.

Address reprint requests to Dr. Lukas Tamm, Department of Molecular Physiology and Biological Physics, University of Virginia School of Medicine, Health Sciences Center, Box 449, Charlottesville, VA 22908. Tel.: 804-982-3578; Fax: 804-982-1616; E-mail: lkt2e@virginia.edu.

© 1996 by the Biophysical Society

0006-3495/96/05/2275/12 $2.00

tween vesicles at mildly acidic but not at neutral pH. Other studies have compared the interactions of wild-type and mutant fusion peptides with lipid model membranes. Wharton et al. (1988) compared 20- and 23-residue peptides corresponding to wild-type and three single-site mutant HAs. These were the G1E and G4E mutations that were used by Gething et al. (1986) and the ΔG1 variant of HA2, which lacked the N-terminal glycine (Garten et al., 1981). The corresponding peptide analogs exhibited fusion properties toward liposomes similar to those of their whole HA counterparts toward cell membranes. The same series of peptides revealed a correlation between surface activity and fusogenicity (Burger et al., 1991). Using surface activity, circular dichroism (CD) spectroscopy, tryptophan fluorescence, and leakage of liposomal contents on the wild-type, G1E, and G4E peptides, Rafalski et al. (1991) also found that surface activity and content leakage correlated with fusogenicity. More recently, Steinhauer et al. (1995) have extended their studies with the synthesis of several new fusion peptide mutants and the introduction of the analogous mutations into the full-length HA. Two of these peptides address the positional specificity of the N-terminal glycine: the GALF and AGLF peptides contain an insertion of an alanine between glycine-1 and leucine-2 or have an alanine appended to the N-terminus, respectively. In hemolysis assays, the AGLF peptide exhibited activity similar to that of the wild-type peptide, whereas the GALF showed significantly lower activity. Taken together, the studies on the mutations in the fusion peptide region demonstrate that the positions of the first two glycines in this sequence are important for the fusogenicity of both the hemagglutinin and the derived synthetic fusion peptides. However, a clear correlation between the fusogenicity of fusion peptides and their structure in lipid bilayers has not yet been found.

In this work, we have designed experiments to test whether the secondary structures and orientations of the fusogenic peptides are different from the nonfusogenic ones and/or whether the fusogenic peptides alter the lipid bilayer structure in a fashion different from that of the nonfusogenic peptides. The sequences of the peptides of this study are given in Fig. 1. They correspond to the mutations and the variant described by Gething et al. (1986), Steinhauer et al. (1995), and Garten et al. (1981), respectively. All peptides are quite hydrophobic, negatively charged, and glycine-rich and can potentially form amphiphilic α-helices. Attenuated total reflection-Fourier transform infrared (ATR-FTIR), CD, and fluorescence spectroscopies are used to compare interactions and structures of these peptides in lipid bilayers.

MATERIALS AND METHODS

Materials

1-Palmitoyl-2-oleoylphosphatidylcholine (POPC) and dimyristoylphosphatidylcholine (DMPC) were purchased from Avanti Polar Lipids (Alabaster, AL) and used without further purification. Peptides were made by the F-moc procedure (Atherton and Sheppard, 1985) on an Applied Biosystems 430A peptide synthesizer. They were ~98% pure, as judged by high-performance liquid chromatography on a C_{18} column using a 10–60% MeCN gradient. The correct sequence was checked by mass spectrometry and amino acid sequencing of the four terminal residues. Peptide concentrations were determined by quantitative amino acid analysis. All other chemicals were from Sigma (St. Louis, MO), Fisher (Fair Lawn, NJ), or Eastman Kodak (Rochester, NY) and were of the highest available purity.

Preparation of vesicles

To prepare unilamellar vesicles, 0.5 μmol of POPC or DMPC in chloroform was mixed with an appropriate volume of peptide dissolved in dimethyl sulfoxide (DMSO) to obtain the desired peptide-to-lipid ratio. The solvent was evaporated under a stream of nitrogen, the dried lipid-peptide mixture was subjected to a high vacuum for at least 1 h to remove trace amounts of solvent, and 0.5 ml of phosphate buffered saline (10 mM NaP_i, 150 mM NaCl, pH 7.4) was added. Uniformly sized, unilamellar vesicles to be used for the preparation of supported planar bilayers were prepared by extrusion through 100-nm pore diameter polycarbonate membranes (Nucleopore, Pleasanton, CA), using a syringe-type Liposofast extruder (Avestin, Ottawa, ON). Small unilamellar vesicles (SUVs) to be used for CD and fluorescence spectroscopy were prepared by sonication in a Branson tip probe sonicator for 45 min at 50% duty cycle.

Preparation of supported bilayers

Planar phospholipid bilayers supported on germanium ATR plates were prepared as previously described (Frey and Tamm, 1991). Briefly, a monomolecular film of POPC or DMPC dissolved in a 9:1 (v/v) hexane/ethanol mixture was spread at the surface of an aqueous buffer (10 mM Tris-acetic acid, 0.002% NaN_3, pH 5.0) in a circular Fromherz trough (Mayer, Göttingen, Germany). The cleaned germanium plate (50 × 20 × 1 mm^3 with 45° beveled edges; Spectral Systems, Irvington, NY) was immersed vertically through the monolayer and withdrawn at a lower speed, with the surface pressure of the monolayer held constant (32 mN/m). The plate was assembled in the measuring cell, and the suspension of extruded vesicles with or without incorporated peptide was injected into the cell and incubated at room temperature for 2 h to allow the vesicles to fuse with the monolayer, yielding supported bilayers on both sides of the germanium plate. Excess unfused vesicles and unbound peptides were flushed with 6 ml of D_2O buffer (5 mM HEPES, 10 mM 2-(*N*-morpholino)ethanesulfonic acid, 135 mM NaCl in D_2O; pH adjusted to 7.4 or 5.0 with NaOH) before the spectra were recorded.

Infrared spectroscopy

Polarized infrared spectra were recorded on a Nicolet 740 Fourier-transform infrared spectrometer as described (Tamm and Tatulian, 1993). The

Peptide	Sequence (1 10 20)	n_{res}	Fusogenicity	Net Charge
wt -23	GLFGAIAGFIENGWEGMIDGWYG	23	+	-3
G1E	ELFGAIAGFIENGWEGMIDGWYG	23	-	-4
ΔG1	LFGAIAGFIENGWEGMIDGWYG	22	-	-3
GALF	GALFGAIAGFIENGWEGMIDGWYG	24	-	-3
AGLF	AGLFGAIAGFIENGWEGMIDGWYG	24	+	-3

FIGURE 1 Sequences, numbers of residues (n_{res}), fusogenicities, and net charges of the wild-type influenza hemagglutinin fusion peptide (strain X31) and four derived mutant peptides. The fusogenicities refer to a cell-to-cell fusion assay with cells expressing recombinant HA with N-terminal HA2 sequences as shown and to measurements of hemolysis with the shown synthetic peptides (Steinhauer et al., 1995). Bold letters correspond to charged and hydrophilic residues.

instrument was purged with nitrogen for 2 h to remove H_2O vapor. ATR-FTIR spectra of supported bilayers were recorded at pH 7.4 and 5.0 with parallel and perpendicular polarized infrared light; 2000 scans were collected at each polarization with a nominal resolution of 2 cm^{-1}. ATR spectra of D_2O buffers of respective pH and polarization were used as references in converting transmittance spectra to absorbance spectra.

Processing of infrared spectra and order parameter calculations

The spectra were baseline corrected, and contributions of residual H_2O vapor were subtracted. To resolve overlapping bands, the spectra were processed using Lab Calc software (Galactic Industries, Salem, NH). Second-derivative spectra were calculated to identify the positions of the component bands in the spectra. These wavenumbers were used as initial parameters for curve fitting with Gaussian component peaks. Curve fitting was considered satisfactory when 1) the resulting bands shifted by no more than 2 cm^{-1} from the original positions, 2) all component peaks had reasonable half-widths (<20–25 cm^{-1}), and 3) good agreement between the calculated sum of all components and the experimental spectra was achieved ($\chi^2 < 10^{-6}$).

To determine order parameters, the ATR dichroic ratios ($R^{ATR} = A_\parallel/A_\perp$) of the lipid and peptide bands of interest were calculated by dividing the absorbances at parallel and perpendicular polarizations of the infrared light. The dichroic ratio is related to an orientational order parameter,

$$S = (3\langle\cos^2\theta\rangle - 1)/2, \quad (1)$$

where θ represents the angle that the molecular director (e.g., the main axis of an α-helix or a lipid hydrocarbon chain) forms with the bilayer normal. The angular brackets denote a time and space average over all angles in the sample during the characteristic time of the IR experiment. Order parameters that describe the orientational distributions of the lipid hydrocarbon chains, S_L, and the amide I transition dipole moments, $S_{\text{amide I}}$, were calculated from the R^{ATR} values as previously described (Frey and Tamm, 1991; Tamm and Tatulian, 1993):

$$S_L = -2\frac{E_x^2 - R^{ATR}E_y^2 + E_z^2}{E_x^2 - R^{ATR}E_y^2 - 2E_z^2} \quad (2)$$

$$S_{\text{amide I}} = \frac{E_x^2 - R^{ATR}E_y^2 + E_z^2}{E_x^2 - R^{ATR}E_y^2 - 2E_z^2}. \quad (3)$$

In Eqs. 2 and 3, E_x, E_y, and E_z are the Cartesian components of the electric field amplitude at the germanium-buffer interface. For the conditions used in this and our previous work, and ignoring possible small changes due to dispersion in the spectral region of interest, $E_x^2 = 1.9691$, $E_y^2 = 2.2486$, and $E_z^2 = 1.8917$ (Tamm and Tatulian, 1993). Because the amide I transition dipole moments of residues participating in a helix are distributed symmetrically around the helix long axis, one can calculate an order parameter, S_H, which describes the orientational distribution of the helices in the lipid bilayer (Frey and Tamm, 1991):

$$S_H = \frac{2S_{\text{amide I}}}{f_H(3\cos^2\alpha - 1)} = (1.97/f_H)S_{\text{amide I}}, \quad (4)$$

where α is the angle the transition dipole moment forms with the helix long axis and f_H denotes the fraction of residues in α-helices. Values ranging between 29° and 41° have been reported for α in the literature (Miyazawa and Blout, 1961; Bradbury et al., 1962; Tsuboi, 1962). In this work, we take α as 35° and discuss the effect that larger or smaller values of α would have on the reported order parameters. Unless they form a β-barrel, the amide I transition moments in β-strands are not distributed axially symmetrically about any of the three principal axes of a β-strand or β-sheet. Therefore, no analog to Eq. 4 exists for the most general case of β-structures (Rodionova et al., 1995).

Fluorescence spectroscopy

Fluorescence measurements were performed on a SPEX spectrofluorometer (SPEX Industries, Edison, NJ) at 20°C. The spectra of sonicated vesicles were recorded at a peptide concentration of about 40 μM and a peptide-to-lipid molar ratio of 1:10. Tryptophan emission spectra were recorded using an excitation wavelength of 285 nm. Bandwidths of 4.25 nm were used in the excitation and emission pathways. The fluorescence intensities were corrected for light scattering and signal arising from sources other than tryptophan by subtracting spectra obtained with vesicles of identical lipid composition and concentration, but without peptide.

Circular dichroism spectroscopy

Circular dichroism measurements were performed on a Jasco 700 CD spectrometer (Jasco, Rochester, NY). The spectra of sonicated vesicles were recorded at peptide concentrations of about 35 μM and a peptide-to-lipid molar ratio of 1:10. The actual concentrations of each sample were determined by measuring the absorbance at 285 nm of a small aliquot that was diluted into DMSO and relating the measured value to that of a standard sample of known concentration in DMSO. Each CD spectrum was obtained by averaging three scans that were recorded at a rate of 2 nm/s between 190 and 250 nm. All samples were measured in a temperature-controlled 1.0-mm-pathlength cell at 20°C. The CD spectra were corrected for signal arising from sources other than peptide by subtracting spectra obtained with vesicles of identical composition and concentration, but without peptide.

RESULTS

Tryptophan fluorescence of the peptides bound to lipid bilayers

To demonstrate binding of the peptides to lipid bilayers and to obtain a qualitative comparison of the average polarity of the microenvironment of the tryptophans under different conditions, we measured tryptophan fluorescence emission spectra of the peptides of Fig. 1 (note tryptophans in positions 14 and 21) in 6 M urea and when bound to vesicles of different lipid composition at pH 7.4 and 5. The fluorescence emission of tryptophan is sensitive to the polarity of its environment; generally, the emission maximum shifts to shorter wavelength for more apolar environments. Fig. 2 shows the emission spectra for wt-23 in 6 M urea and when bound to vesicles of POPC or POPC/cholesterol (7:3) at pH 7.4 or 5. In Table 1, the emission maxima of the mutant peptides under the various conditions are compiled. When dissolved in 6 M urea, all five peptides exhibited emission maxima at 361 or 362 nm, independent of the pH. A blue shift occurred for all peptides when they were bound to lipid vesicles. The blue shift was at maximum when the peptides were bound to POPC vesicles at pH 5. The emission maximum under these conditions was at 343 to 344 nm for all peptides. Smaller blue shifts, which depended on the sequence of the peptides, were observed in vesicles of POPC or POPC/cholesterol at pH 7.4. The two fusogenic peptides, wt-23 and AGLF, showed the largest blue shifts, closely followed by GALF, followed by G1E and ΔG1. These data indicate that all peptides bind to lipid vesicles at pH 7.4 and 5 and that the fusogenic peptides

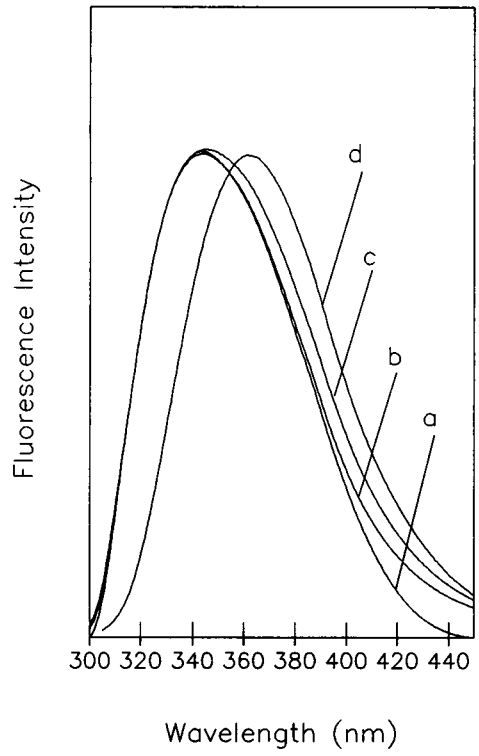

FIGURE 2 Fluorescence emission spectra of the wild-type fusion peptide, wt-23, in 6 M urea (*d*) or bound to small unilamellar vesicles of POPC (*a* and *b*) or POPC/cholesterol (7:3) (*c*) at 20°C. Spectrum *a* was measured in pH 5 buffer. All other spectra were measured in pH 7.4 buffer. Excitation was at 285 nm, using 4-nm slits in the excitation and emission paths. Peptide and lipid concentrations were 40 μM and 0.4 mM, respectively.

may probe slightly more apolar environments at pH 7.4 than the nonfusogenic peptides. Qualitatively similar spectra were obtained when wt-23 was bound to small unilamellar vesicles of DMPC. When these vesicles were suspended in pH 5 buffer, the emission maximum was at 343 nm and did not change as a function of temperature between 20 and 24°C (data not shown).

Secondary structure and orientation of the peptides in lipid bilayers

A combination of CD and FTIR spectroscopy was used to elucidate the secondary structure of the peptides inserted into lipid bilayers and the orientation of the helical segments of the peptides within these bilayers. Far-UV CD spectra of the five peptides in POPC vesicles at pH 5 are shown in Fig. 3. Measurements of the molar ellipticities at 222 nm yielded -12.9, -7.1, -5.1, -2.2, and -0.8×10^3 degree cm^2/dmol for wt-23, AGLF, G1E, ΔG1, and GALF, respectively. If a molar ellipticity of -30×10^3 degree cm^2/dmol at 222 nm is taken to represent 100% helical secondary structure (Yang et al., 1986), our CD data indicate that the fusogenic peptides, wt-23 and AGLF, contained 43% and 24% helix, respectively, whereas G1E exhibited only 17% and GALF and ΔG1 <10% helix at pH 5 (Table 2). At pH 7.4, wt-23 and AGLF were also more helical than the other three peptides, and 30 mol % cholesterol had little effect on the helicity of any of the peptides used in this study (data not shown). The shapes of the spectra of all five peptides also indicate the presence of β-structure. However, the lack of useful spectral information below 200 nm did not allow us to quantitate the relative content of β-structure from these spectra.

The secondary structures of the peptides in lipid bilayers was further investigated by FTIR spectroscopy. Polarized ATR-FTIR spectra of the wild-type and mutant fusion peptides in the region between 1680 and 1600 cm^{-1} at pH 7.4 and 5 are presented in Fig. 4. This region contains the amide I′ band, which is sensitive to the secondary structure of the peptides. Decomposition of the amide I′ band consistently yielded two distinct components, one at 1647–1654 cm^{-1} and the other at 1627–1631 cm^{-1}. In some cases a small third band at ~1610 cm^{-1} was observed that is attributed to side-chain vibrations. The component at ~1630 cm^{-1} represents the fraction of residues in β-strand conformation (Byler and Susi, 1986; Surewicz and Mantsch, 1988; Surewicz et al., 1993; Arrondo et al., 1993; Goormaghtigh

TABLE 1 Fluorescence emission maxima of the wild-type and mutant fusion peptides in urea and bound to lipid bilayers at pH 7.4 and 5.0

	λ_{max} (nm)			
Peptide	Urea, pH 7.4 or 5.0	POPC/Ch (7:3), pH 7.4	POPC, pH 7.4	POPC, pH 5.0
wt-23	362	347	345	343
G1E	362	352	348	344
ΔG1	362	356	353	343
GALF	361	350	347	343
AGLF	361	351	346	343

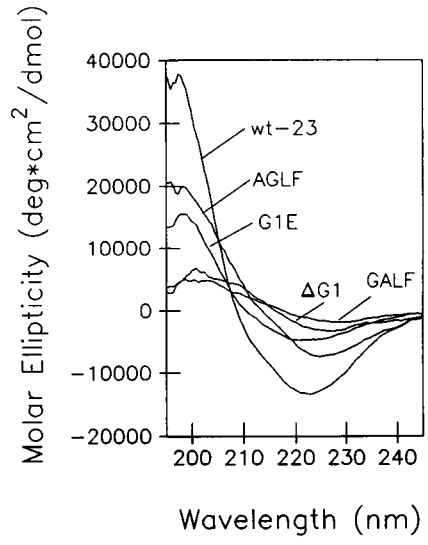

FIGURE 3 Circular dichroism spectra of the wild-type and mutant fusion peptides bound to small unilamellar vesicles (SUVs) of POPC at pH 5 and measured at 20°C. Peptide and lipid concentrations were 35 μM and 0.35 mM, respectively.

TABLE 2 Estimates of α-helical and β-pleated secondary structures of the various peptides in POPC bilayers at pH 5.0

Peptide	% α-Helix*	% β-Structure‡	Other§
wt-23	43	27	30
AGLF	24	55	21
GALF	<10	61	30
ΔG1	<10	58	30
G1E	17	58	25

*From CD on small unilamellar vesicles.
‡From FTIR on planar membranes.
§Not assigned as α-helix or β-structure by CD or FTIR spectroscopy.

et al., 1994). The component at ~1650 cm^{-1} is due to residues in α-helices and irregular secondary structures. Even when most of the amide protons of the irregular structure are exchanged with deuterons, it is difficult, at the present signal-to-noise ratios, to distinguish between α-helical and irregular secondary structures because the amide I′ bands of these two structures are not well separated (Byler and Susi, 1986; Surewicz and Mantsch, 1988; Surewicz et al., 1993; Arrondo et al., 1993; Goormaghtigh et al., 1994). Therefore, we used the amide I′ bands to calculate only the relative amounts of β-structure of the peptides by dividing the integrated area of the component at about 1630 cm^{-1} by that of the whole amide I′ band, excluding the small side-chain component. wt-23 exhibited ~27% β-structure, and the mutant peptides averaged at about 50–60% β-structure when bound to planar POPC bilayers at pH 5. Similar percentages of β-structure were obtained at pH 7.4. We estimate from multiple experiments (three to five for each peptide) that our determinations of the secondary structure from ATR-FTIR spectroscopy contain an error of approximately ±10%. This figure also includes a small, but persistent, deviation in secondary structures derived from parallel and perpendicular polarized spectra. The combined results of the secondary structure measurements by CD and ATR-FTIR spectroscopy at pH 5 are summarized in Table 2.

Polarized ATR-FTIR spectra of wt-23 and G1E were also recorded in DMPC bilayers at pH 7.4 and 5 (data not shown). These spectra were very similar to those shown in Fig. 4 for the same peptides in POPC. This is not surprising, because supported bilayers of DMPC are thought to be composed of coexisting domains of lipid in the gel and liquid-crystalline phases at our measuring temperature of 21–22°C (Tamm, 1988; Tatulian et al., 1995b; Rodionova et al., 1995) and because most peptides and proteins preferentially partition into the liquid-crystalline phase when they have a choice between these two lipid phases. We believe that this is also the case for the fusion peptides of this study, because position and intensity of the tryptophan fluorescence emission of wt-23 in DMPC vesicles did not change in the 20–24°C temperature interval. The relative contents of β-structure and α-helix were calculated for wt-23 and G1E in DMPC from the FTIR and CD spectra. In addition, order parameters, which are functions of the orientational distributions of the helices and β-strands of wt-23 and G1E in bilayers of DMPC, were determined from the dichroic ratios of the individual component peaks (Table 3).

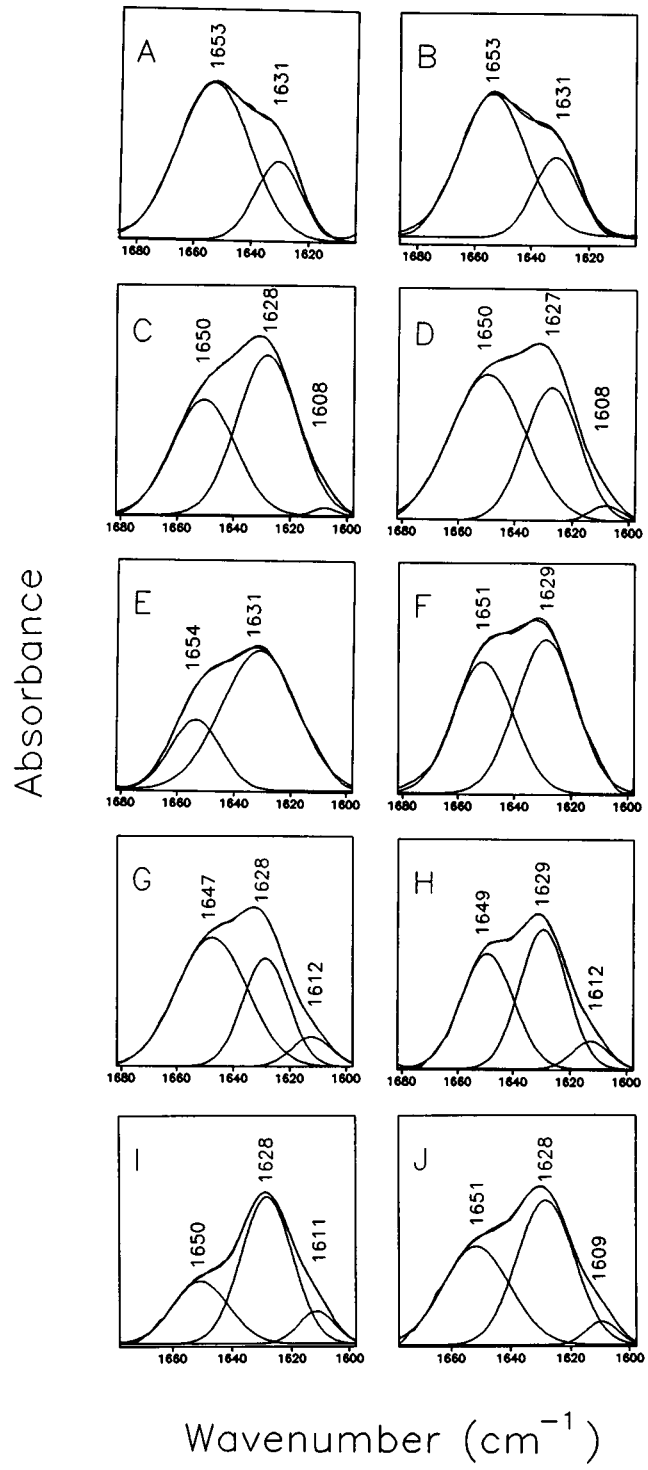

FIGURE 4 Parallel polarized ATR-FTIR spectra in the amide I region of wt-23 (*A* and *B*), AGLF (*C* and *D*), ΔG1 (*E* and *F*), GALF (*G* and *H*), and G1E (*I* and *J*) peptides in POPC bilayers at pH 7.4 (*left*) and pH 5.0 (*right*), and their decompositions. The spectra were decomposed using Gaussian component lineshapes as described in Materials and Methods.

TABLE 3 Secondary structure and orientation of the WT-23 and G1E peptides in DMPC bilayers from FTIR and CD spectroscopy at pH 7.4 and 5*‡

	wt-23		G1E	
	pH 7.4	pH 5	pH 7.4	pH 5
% β-structure	39	33	56	58
R^{ATR}_{1630}	5.2 ± 1.1	4.1 ± 1.7	3.1 ± 0.6	2.9 ± 0.7
$S^{\beta}_{amide\ I}$	$0.58^{+0.06}_{-0.09}$	$0.49^{+0.13}_{-0.28}$	$0.35^{+0.09}_{-0.11}$	$0.31^{+0.12}_{-0.16}$
% α-helix§	50	43	21	17
f_H¶	0.82	0.64	0.48	0.40
R^{ATR}_{1653}	2.1 ± 0.2	2.1 ± 0.3	—	—
$S^{\alpha}_{amide\ I}$	$0.13^{+0.05}_{-0.06}$	$0.13^{+0.08}_{-0.10}$	—	—
S_H	$0.32^{+0.13}_{-0.16}$	$0.41^{+0.25}_{-0.30}$	—	—

*The data are averaged from five independent experiments for wt-23 and three independent experiments for G1E.
‡The errors in S are not distributed symmetrically about the mean, because of the functional dependence of S on R^{ATR}.
§From CD spectroscopy.
¶Ratio of residues in α-helical conformation divided by the sum of residues in α-helical and irregular conformation.

wt-23 contained ~33% β-structure in DMPC at pH 5, and the order parameter describing the orientational distribution of the amide I transition dipole moments of the β-strand component, $S^{\beta}_{amide\ I}$, of this peptide was 0.49 (0.21–0.62) (because of the nonlinear dependence of S on R^{ATR}, the errors are not distributed symmetrically about the mean, i.e., given the experimental error of R^{ATR}_{1630}, $S^{\beta}_{amide\ I}$ could assume values betwen 0.21 and 0.62 for wt-23 at pH 5.0). At pH 7.4, wt-23 contained ~39% β-structure and $S^{\beta}_{amide\ I}$ was 0.58 (0.49–0.64), i.e., not significantly different from those obtained at pH 5. This peptide also contained ~43% α-helix (~50% at pH 7.4), the orientational distribution of which was described by an order parameter, S_H, of 0.41 (0.11–0.66) and 0.32 (0.16–0.45) at pH 7.4 and 5.0, respectively. As will be discussed in more detail below, these values indicate that, in all likelihood, both elements of secondary structure of this peptide were inserted into the lipid bilayer at oblique angles. The G1E peptide contained more β-structure (~57% irrespective of pH) than wt-23, and $S^{\beta}_{amide\ I}$ was 0.31 (0.15–0.43) at pH 5 and 0.35 (0.24–0.44) at pH 7.4. Because of the small fraction of α-helix (~20%) in G1E, we were not able to reliably determine the orientation of this secondary structure element in the lipid bilayer.

Effects of the peptides on the lipid bilayer

The positions and dichroic ratios of the lipid methylene symmetric and antisymmetric stretching vibrations are sensitive to the structure and packing of the lipid hydrocarbon chains. Therefore, effects of wt-23 and G1E on this region of the IR spectra were investigated. Fig. 5 shows polarized ATR-FTIR spectra of the methylene stretching region of DMPC with and without 10 mol% incorporated wt-23 at pH 5. These spectra contain two major peaks at approximately 2921 and 2852 cm^{-1}, which correspond to the antisymmetric and symmetric methylene stretching vibrations, respectively. The symmetric methylene stretching frequency is intermediate to that found for hydrocarbon chains in the gel and liquid-crystalline states (2849–2850 and 2854 cm^{-1}, respectively; Mantsch and McElhaney, 1991), indicating that these bilayers were indeed in a region of coexisting solid and fluid lipids at room temperature. These wavenumbers were not significantly affected by the presence of any of the peptides in the bilayer. To determine the orientational order of the lipid hydrocarbon chains in the supported bilayers, the dichroic ratios of the methylene stretching

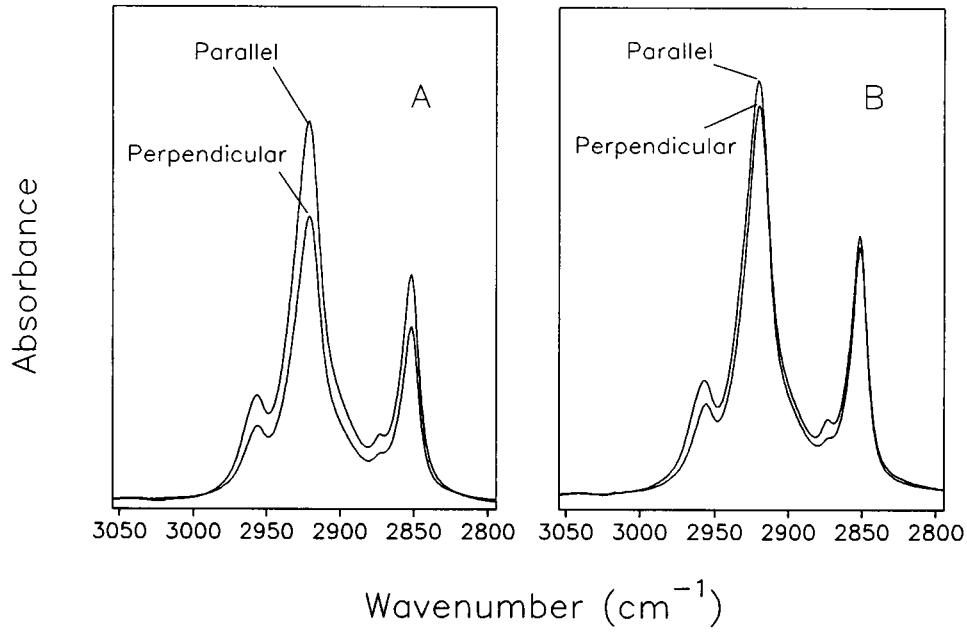

FIGURE 5 Polarized ATR-FTIR spectra in the methylene stretching region of pure DMPC bilayers (*A*) and DMPC bilayers containing 10 mol% wt-23 fusion peptide (*B*) at pH 5. Spectra recorded with parallel and perpendicular polarized infrared light are shown as indicated.

vibrations were calculated from the polarized ATR-FTIR spectra of Fig. 5. These values were 1.29 ± 0.06 and 1.05 ± 0.02 for DMPC in the absence and presence, respectively, of 10 mol% wt-23. The corresponding order parameters, calculated according to Eq. 2, were 0.41 ± 0.07 and 0.72 ± 0.06 in the absence and presence, respectively, of peptide. Apparently, the lipids became more ordered when the fusion peptide was inserted into the bilayers. This effect was studied as a function of the peptide-to-lipid ratio in the bilayer. Fig. 6 shows that the lipid order parameter increased rapidly when only small amounts of fusion peptide were incorporated. The effect of the mutant peptide G1E was very similar to that of the wild-type peptide.

Another region of interest in the FTIR spectra is the ester carbonyl stretching vibration of the lipids in the bilayer at around 1735 cm^{-1} (Fig. 7). This band is known to be composed of two component bands centered near 1740 and 1727 cm^{-1} (Levin et al., 1982; Mendelsohn and Mantsch, 1986). The two components are thought to correspond to free and hydrogen-bonded carbonyl groups, respectively. It has further been shown by selective isotopic replacement of the carbonyl carbon with ^{13}C that the carbonyl groups of both fatty acyl chains in phospholipids contribute about equally to the two spectral components (Blume et al., 1988; Lewis et al., 1994). Therefore, the carbonyl groups of the sn-1 and sn-2 chains can both participate in hydrogen bonding, presumably with interfacial water. Ordinarily, decomposition of the spectral region between about 1700 and 1760 cm^{-1} is necessary to observe the splitting of the band into two distinguishable components. This is the case for pure POPC or DMPC bilayers in the absence of peptide (not shown), as well as for POPC bilayers containing 10 mol% of the two fusogenic peptides wt-23 (Fig. 7 *A*) and AGLF (not shown). The two nonfusogenic peptides ΔG1 and G1E exhibit a split carbonyl peak, which for the case of G1E is readily visible even before spectral decomposition (Fig. 7 *C*). The lipid ester carbonyl band in the presence of GALF in POPC (Fig. 7 *B*), although broadened, looks more like that in the presence of the two fusogenic peptides, but this peptide is also mildly fusogenic, as assayed by red blood cell lysis at very high peptide concentrations (Steinhauer et al., 1995). The carbonyl bands of the spectra of bilayers

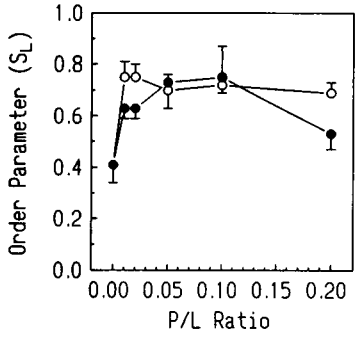

FIGURE 6 Lipid order parameter as a function of the peptide-to-DMPC ratio for the wt-23 (○) and G1E (●) fusion peptides at pH 5.

containing 10 mol % wt-23, AGLF, or GALF are readily resolved into the two expected components at about 1741 and 1728 cm^{-1} (Fig. 7, *A* and *B*). Two factors contribute to the carbonyl band splitting in the presence of ΔG1 and G1E. Spectral decomposition reveals that high concentrations of these peptides caused 1) a larger separation and 2) a decrease in the apparent bandwidths of the component bands (Fig. 8). The high and low component frequencies gradually changed over a peptide concentration range from zero to 1:5 peptide-to-lipid ratio. The maximum change was +4.5 cm^{-1} for the high-frequency component and −4 cm^{-1} for the low-frequency component. The bandwidths of both component bands were decreased by 2–3 cm^{-1} over the concentration range that was studied.

DISCUSSION

The present work confirms and extends previous studies on the secondary structure of the influenza hemagglutinin fusion peptide in lipid bilayers. A major new result of this work is that a series of peptides that are all derived from the extreme N-terminus of the HA2 chain of influenza HA (strain X31) contain significant amounts of β-structure. Our FTIR experiments indicate that the wild-type sequence (wt-23) contains ~30% β-structure, whereas several mutant peptides with single or double amino acid replacements exhibited 50–60% β-structure. Most previous studies used strictly CD spectroscopy to determine the secondary structure of fusion peptides in lipid bilayers. In the absence of reliable spectral information extending to at least 190 nm, it is essentially impossible to quantify secondary structures other than α-helix from CD spectra. The noise introduced by vesicle-induced light scattering precluded the collection of reliable CD data below 200 nm; hence β-structure has not been previously identified in these peptides. The combination of FTIR sectroscopy with CD spectroscopy (summarized in Table 2) allowed us to circumvent this limitation: the amide I′ component band corresponding to β-structure is well resolved and hence easily quantitated in FTIR spectroscopy, and the relative content of residues in α-helical conformation is most easily determined in CD spectroscopy, because the molar ellipticity at 222 nm is dominated by the helical signal.

Our CD and FTIR experiments suggest that helicity correlates weakly with fusogenicity and that high contents of β-structure are inhibitory to fusion, as the wt and, to a lesser extent, AGLF peptides exhibited the highest helical and lowest β-structure contents. The contents of α-helix given in Table 2 are in reasonable agreement with previously reported values. Lear and DeGrado (1987) found that a 20-residue wt peptide corresponding to the B/Lee strain HA contained ~55% α-helix when inserted into large unilamellar vesicles of POPC at pH 5. Rafalski et al. (1991) found that 20-residue peptides corresponding to the wt and G1E peptides from X-31 strain HA contained ~66% and 40% α-helix, respectively, when inserted into SUV of POPC at

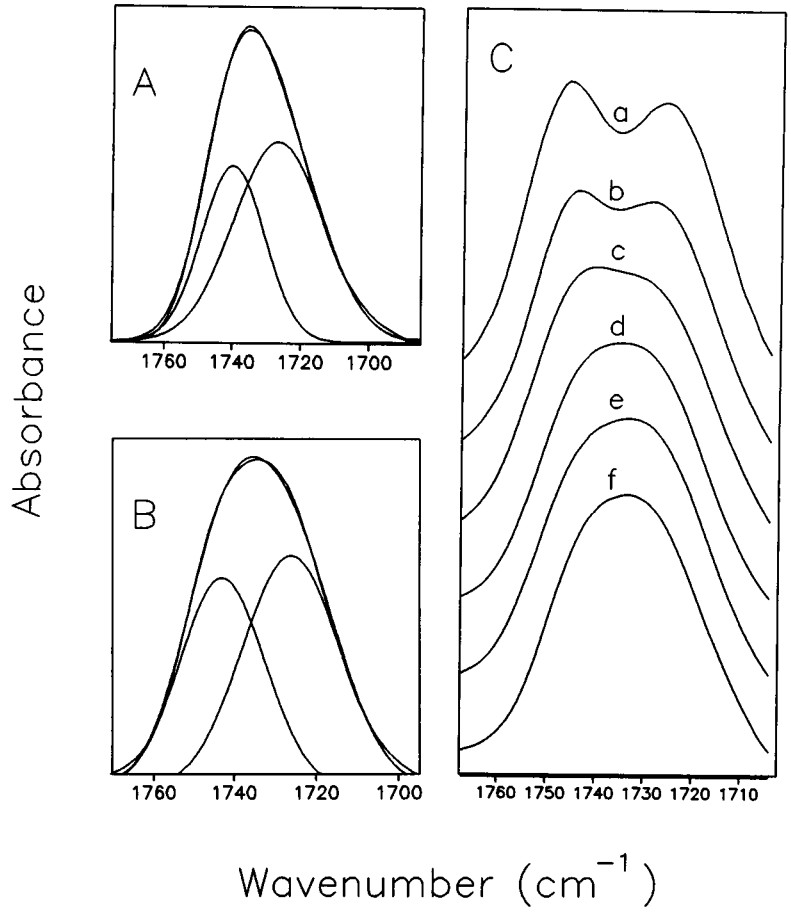

FIGURE 7 Lipid ester carbonyl stretching region of parallel polarized ATR-FTIR spectra of wt-23 (*A*), GALF (*B*), and G1E (*C*) peptides in POPC bilayers at pH 7.4. In *A* and *B*, the peptide-to-lipid ratios are 1:5, and the decompositions into two components are shown as explained in the text. In *C*, the effect of increasing concentrations of G1E in the bilayer is shown. The peptide-to-lipid ratios are 1:5 (*a*), 1:10 (*b*), 1:20 (*c*), 1:50 (*d*), 1:100 (*e*), and pure POPC (*f*).

pH 5. Wharton et al. (1988) reported that wt-23, i.e., the same peptide used in this study, contained ~50% α-helix, and that 20 residue peptides containing the G1E substitution and the ΔG1 deletion contained ~25% and 20% α-helix, respectively, when inserted into SUV of POPC at pH 5. In the absence of more systematic studies, it is difficult to assess whether the observed differences are due to the small differences in the sequences, lengths of the peptides, or the types of vesicles used.

Having identified α- and β-structure in fusion peptides, one might ask, which of the two determines the fusogenic activity of these peptides? A minimum number of residues in α-helical conformation appears to be important for the fusion activity of the influenza HA fusion peptide. However, this does not rule out the possibility that a certain amount of β-structure is important as well. For example, a balance between α- and β-structure seems to exist in the fusion peptide of gp41 of HIV that depends on various parameters such as the peptide-to-lipid ratio, the specific peptide sequence, and the presence or absence of divalent cations and negatively charged lipids in the membrane (Rafalski et al., 1990; Gordon et al., 1992; Martin et al., 1993; Nieva et al., 1994). Interestingly, a recent study of the putative fusion peptide of fertilin (PH-30), the fusion protein of the sperm cell surface, exhibited a large amount of β-structure in lipid bilayers (Muga et al., 1994), even though this sequence was modeled as a sided membrane-interactive α-helix in analogy with many viral fusion peptides (Blobel et al., 1992). Therefore, it is possible that one of the main characteristics of functional fusion peptides is that they can adopt α- and β-structures, simultaneously in different segments of the sequence, and/or change their conformation in response to environmental changes. Although we cannot directly assign specific segments of the fusion peptides to α- or β-structures, inspection of the sequence by secondary structure prediction routines and hydrophobic moment calculations indicates that the N-terminus has a higher propensity for β-structure and the C-terminus more likely forms an amphiphilic α-helix.

The ATR-FTIR results also provide information pertaining to peptide orientation relative to the plane of the lipid bilayer. The order parameters of the helical and β-strand components presented in Table 3 are intermediate between the extrema of 1.0 and −0.5 (corresponding to orientations parallel and perpendicular to the membrane normal, respectively). Therefore, orientations of either segment exclusively parallel or perpendicular to the membrane can be excluded. Because of the time and space averaging of the $\langle\cos^2\theta\rangle$ term in the definition of the order parameter (Eq. 1), a unique orientation or orientational distribution cannot be given. However, if some extremely peculiar distributions are excluded, it is clear that only orientational distributions

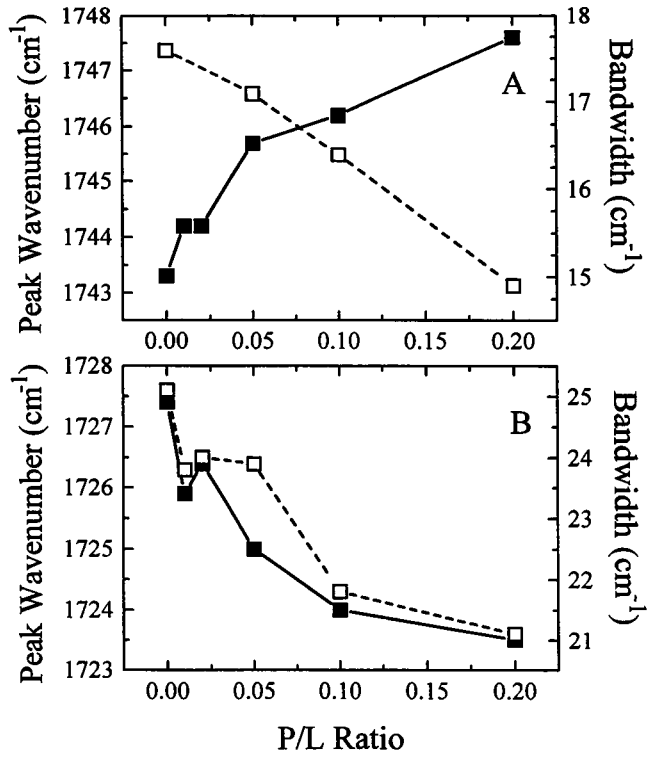

FIGURE 8 Peak wavenumbers (■) and bandwidths (□) of the higher (*A*) and lower (*B*) frequency components of the ester carbonyl stretching band of POPC as a function of increasing concentrations of the G1E fusion peptide in the lipid bilayer.

with signficiant oblique components of both secondary structures are consistent with the data. (In principle, it is possible that bimodal distributions with approximately 67% of the elements aligned parallel and 33% elements aligned perpendicular to the membrane normal could yield an order parameter of ~0.5.) If the orientational distribution were a monodisperse δ-function (chosen for illustrative purposes), the helical order parameter of wt-23 at pH 5.0 (0.41 (0.11–0.66)) would correspond to an angle of 39° (28–50°) for the orientation of the helix from the membrane normal. Similarly, the amide I′ transition moments of the β-structure (which make an angle of about 20° with the peptide carbonyl bond; Fraser and MacRae, 1973; Krimm and Bandekar, 1986) are oriented at 30–50° to the membrane normal under these conditions ($S^{\beta}_{\text{amide I}}$ = 0.15–0.62), without any significant difference between the wt-23 and G1E peptides. The similarity of the order parameters calculated for the helical segment and the β-strand carbonyl groups of the wt-23 peptide imply that their average orientations may be similar.

For the calculation of helical and β-strand parameters, the primary data yield an order parameter of the amide I transition moment, $S^{\alpha}_{\text{amide I}}$ and $S^{\beta}_{\text{amide I}}$, respectively. The major uncertainties for calculating these values are the experimental uncertainties resulting from repeated measurements of R^{ATR} (Miyazawa and Blout, 1961; Bradbury et al., 1962; Tsuboi, 1962). (Minor uncertainties may be associated with the assumed values for the refractive indices; see Tamm and Tatulian, 1993, for references.) For the case of β-strands (or β-sheets) the analysis cannot be carried any further because of the lack of cylindrical symmetry of these structures. Several orientations of the β-strand that are cylindrically symmetrical about the axis of the transition moment are possible (see Rodionova et al., 1995). Because the amide I transition moments are distributed symmetrically about the long axis of an α-helix, the helical order parameter, S_H, can be calculated from $S^{\alpha}_{\text{amide I}}$, provided the angle α between the transition moment and the helix is known. In this work we have assumed α = 35°, although values between 29° and 41° have been reported in the literature. For a given ATR dichroic ratio, larger angles α yield higher order parameters that correspond to smaller angles θ between the membrane normal and helical axis. For example, S_H, which was 0.41 (θ = 39°) for wt-23 at pH 5 (α = 35°), could range between 0.32 (θ = 42°) for α = 29° and 0.58 (θ = 32°) for α = 41°. The experimental uncertainty of f_H, i.e., the fraction of α-helical residues that contribute to the amide I band at ~1650 cm^{-1}, is another source of error, which according to our estimates is about ±10%. Because the effect of this error and the uncertainty of α on S_H are relatively small compared to the experimental error of R^{ATR}, it is safe to conclude that S_H is in the range between 0.1 and 0.7, or θ ranges between about 30° and 50° for the wt-23 peptide in the lipid bilayer.

Our results on peptide orientation differ from those of a previous experimental study (Ishiguro et al., 1993) but agree vaguely with previous theoretical calculations (Brasseur et al., 1990). Ishiguro et al. (1993) concluded on the basis of their ATR-FTIR spectroscopic measurements that a 20-residue analog of the wild-type fusion peptide corresponding to A/PR/8/34 strain HA was oriented at 60–70° to the membrane normal, independently of pH and the degree of membrane hydration. However, this orientation was measured in egg PC multibilayers that were dry or only partially hydrated; the degree of hydration in the "wet" multibilayers in these preparations is unclear, as hydration was achieved by providing an atmosphere saturated with D_2O vapor for 4 h. Because the orientation of peptides can be quite sensitive to the degree of hydration and the method of membrane preparation, as was demonstrated for the case of the amphiphilic helix-forming bee venom peptide melittin (Frey and Tamm, 1991), Ishiguro's and our results cannot be directly compared. Brasseur et al. (1990) concluded from their three-dimensional helical moment calculations on the fusion peptides of 10 viruses (influenza HA was not included in their study) that many fusion peptides assume orientations in the range 30–35° to the bilayer normal. However, it should be noted that Brasseur et al. (1990) modeled the peptides as 100% helical, which, based on the current and most previous measurements of secondary structure of the fusion peptides, is an oversimplification.

The fusion peptides exert pronounced effects on the structure of the lipid bilayer. G1E induced splitting of the lipid ester carbonyl stretching vibration that is readily ap-

parent in the raw spectra without spectral decomposition (Fig. 7 *C*). In pure lipid bilayers the two carbonyl stretch components can only be visualized by spectral decomposition. The two components have been assigned to hydrogen-bonded and "free" lipid ester carbonyls (Blume et al., 1988; Lewis et al., 1994). Importantly, the peptide-induced splitting of the lipid ester carbonyl vibration correlates with the β/α secondary structure ratio and correlates negatively with the fusogenicity of the peptide used. The wt-23 and AGLF peptides, which have smaller β/α ratios and which are fusogenic, do not split this band; the G1E and ΔG1 peptides split this band. The GALF peptide is intermediate in all three respects (see Steinhauer et al., 1995, for fusogenicity and hemolysis results). GALF gives rise to a broadened lipid ester carbonyl band (Fig. 7 *B*). Protonated or deuterated side-chain carboxyl groups of glutamic and aspartic acid also absorb in the spectral region above 1700 cm^{-1} (Chirgadze et al., 1975; Venyaminov and Kalnin, 1990). However, these contributions must be small compared to the observed absorbances in this region, because their extinction coefficients are less than two-thirds of the peptide amide I band (Chirgadze et al., 1975; Venyaminov and Kalnin, 1990), only four of the 23 residues of G1E have carboxyl side chains, and the measured absorbances at $\sim$1735 cm^{-1} are typically twice as large as the amide I absorbances at the peptide-to-lipid ratios used in our experiments. For G1E, the position of the high-frequency band, previously ascribed to "free" carbonyl groups, increases, and the position of the low frequency band, previously ascribed to hydrogen-bonded carbonyl groups, decreases monotonically, and the widths of both component bands decrease with increasing peptide-to-lipid molar ratio (Fig. 8). Two different mechanisms can explain these dependencies. First, the G1E peptide may interact directly with the lipid ester carbonyl groups. Because the positions of the component bands reflect details of the electronic environment of the chemical bond that gives rise to a particular vibration, it is possible that a side chain of the G1E peptide, which is capable of hydrogen-bonding with carbonyl groups, directly interacts with one of the lipid ester carbonyls. Protonated (deuterated) forms of side-chain carboxyl groups, such as glu-1, glu-11, glu-15 or asp-19, or asn-12, could act as hydrogen donors in such interactions. Amide protons (deuterons) of unpaired β-strands that appear to be abundant in those peptides that split the lipid carbonyl band could also hydrogen-bond to the lipid carbonyl groups. (Note the absence of the high-frequency counterpart of the amide I band that is attributed to β-structure; a high-frequency β-strand amide I component is usually found in hydrogen-bonded antiparallel sheets only (Byler and Susi, 1986; Surewicz and Mantsch, 1988; Surewicz et al., 1993; Arrondo et al., 1993; Goormaghtigh et al., 1994).) A second possibility is that the nonfusogenic mutant peptides reorganize water molecules at the membrane-water interface such that the hydrogen-bonding strength is decreased with one class but increased with another class of lipid ester carbonyls.

The effects of the wt-23 and G1E peptides on lipid were also investigated by measuring the order parameters of the lipid hydrocarbon chains as a function of peptide-to-lipid molar ratio (Fig. 6). To illustrate, the lipid order parameters for DMPC in the absence of peptide, with 10 mol% wt-23 peptide, and with 10 mol% G1E peptide, are 0.41 $\pm$ 0.07, 0.72 $\pm$ 0.06, and 0.63 $\pm$ 0.04, respectively. Clearly, both peptides restricted the orientational distributions of the hydrocarbon chains in the lipid bilayers in a similar fashion, and no significant difference between the fusogenic and nonfusogenic peptides was detected. The increase of the lipid order parameter as a function of peptide concentration appears to be a special feature of the fusion peptides, because other amphiphilic peptides decrease order parameters determined from ATR-FTIR spectroscopy in supported bilayers (Tamm and Tatulian, 1993). This unexpected result may be related to the displacement or rearrangement of water molecules at the membrane interface in response to the binding of fusion peptides. Dehydration at the surface is well known to increase the phase transition temperature in pure lipid bilayers (McIntosh and Magid, 1993), which is equivalent to an increase of the order of hydrocarbon chains in the hydrophobic core of lipid bilayers.

In summary, the foregoing considerations suggest that peptide fusogenicity correlates with the inability to split the lipid ester carbonyl stretch and that a delicate balance between α- and β-structure exists in functional fusion peptides. Both the fusogenic and the nonfusogenic peptides insert their α-helices (angle measurable in wt-23 only) and β-strands at oblique angles into the lipid bilayer and increase the ordering of the lipid chains. It remains difficult to understand how the N-terminal glycine can exert such profound effects upon peptide secondary structure and peptide-lipid interactions. It is tempting to postulate that the crucial property that dictates fusogenicity is the precise three-dimensional structure assumed by the helical and β-strand components in relation to one another and the consequences this structure has for supramolecular organization. For instance, the fusion peptides may form a cone-shaped structure in the lipid bilayer with a larger cross-section in the hydrocarbon region than in the polar headgroup region. Such structures are known to promote membrane fusion, whereas "inverted cones" are inhibitory to fusion (Chernomordik et al., 1995). Fusogenicity may thus depend on positional specificity as it relates to peptide-peptide interactions in addition to peptide-lipid interactions. This would explain the effects of single-site mutations at the N-terminus if this position in the peptide were crucial to the formation of the tertiary or quaternary structure of the fusion peptide complex in lipid bilayers. The correlation of the ability to split the lipid ester carbonyl with the inability to promote fusion could then be explained as the liberation of peptide groups for interaction with the lipid ester carbonyl groups that otherwise would have been sequestered in intra- or inter-peptide interactions in the case of the fusogenic peptides. These issues raise important questions pertaining to the mechanism of HA-mediated membrane fusion. The

physical origin of the observed increase in lipid order parameter needs to be elucidated. In particular, a precise understanding of the hydration state of a lipid bilayer with incorporated fusogenic and nonfusogenic peptides is needed. Such information, together with a more detailed structural model of the fusion peptides, will help in the understanding of how these peptides assist the merging of two closely apposed lipid bilayers into a single membrane.

Note added in proof: Since this manuscript was submitted, a paper appeared in which the secondary structure and orientation in lipid bilayers of the wild-type 20-residue fusion peptide of A/PR8/34 strain HA was investigated by ATR-FTIR spectroscopy and other methods (Lüneberg et al., 1995). These authors found an orientation of the helical component (~45°) similar to the one reported here. However, they report that only 10% of the fusion peptide was in a β-conformation after unbound peptide was removed by column chromatography. It should be noted that there are significant differences in sample preparation between the two works. Lüneberg et al. dried lipid vesicles onto the germanium plate and measured their spectra on multilamellar films in D_2O vapor. Our spectra were measured on single supported bilayers on germanium that were washed with excess buffer and remained immersed in D_2O buffers at all times.

This work was supported by grants R01 AI30557 and T32 GM08323 from the National Institutes of Health.

REFERENCES

Arrondo, J. L. R., A. Muga, J. Castresana, and F. M. Goñi. 1993. Quantitative studies of the structure of proteins in solution by FTIR spectroscopy. *Prog. Biophys. Mol. Biol.* 59:23–56.

Atherton, E., and R. C. Sheppard. 1985. Solid phase peptide synthesis using *N*-fluorenylmethoxycarbonyl amino acid pentafluorophenyl esters. *J. Chem. Soc. Chem. Commun.* 165–166.

Blobel, C. P., T. G. Wolfsberg, C. W. Turck, D. G. Myles, P. Primakoff, and J. M. White. 1992. A potential fusion peptide and an integrin ligand domain in a protein active in sperm-egg fusion. *Nature.* 356:248–252.

Blume, A., W. Hübner, and G. Messner. 1988. Fourier transform infrared spectroscopy of $^{13}C{=}O$-labeled phospholipids hydrogen bonding to carbonyl groups. *Biochemistry.* 27:8239–8249.

Bodian, D. L., R. B. Yamasaki, R. L. Buswell, J. F. Stearns, J. M. White, and I. D. Kuntz. 1993. Inhibition of the fusion-inducing conformational change of influenza hemagglutinin by benzoquinones and hydroquinones. *Biochemistry.* 32:2967–2978.

Bradbury, E. M., L. Brown, A. R. Downie, A. Elliott, R. D. B. Fraser, and W. E. Hanby. 1962. The structure of the ω-form of poly-β-benzyl-L-aspartate. *J. Mol. Biol.* 5:230–247.

Brasseur, R., M. Vandenbranden, B. Cornet, A. Burny, and J.-M. Ruysschaert. 1990. Orientation into the lipid bilayer of an asymmetric amphipathic helical peptide located at the N-terminus of viral fusion proteins. *Biochim. Biophys. Acta.* 1029:267–273.

Bullough, P. A., F. M. Hughson, J. J. Skehel, and D. C. Wiley. 1994. Structure of influenza haemagglutinin at the pH of membrane fusion. *Nature.* 371:37–43.

Burger, K. N. J., S. A. Wharton, R. A. Demel, and A. J. Verkleij. 1991. The interaction of synthetic analogs of the N-terminal fusion sequence of influenza virus with a lipid monolayer. Comparison of fusion-active and fusion-defective analogs. *Biochim. Biophys. Acta.* 1065:121–129.

Byler, D. M., and H. Susi. 1986. Examination of the secondary structure of proteins by deconvolved FTIR spectra. *Biopolymers.* 25:469–487.

Carr, C. M., and P. S. Kim. 1993. A spring-loaded mechanism for the conformational change of influenza hemagglutinin. *Cell.* 73:823–832.

Chernomordik, L., M. M. Kozlov, and J. Zimmerberg. 1995. Lipids in biological membrane fusion. *J. Membr. Biol.* 146:1–14.

Chirgadze, Y. N., O. V. Federov, and N. P. Trushina. 1975. Estimation of amino acid residue side-chain absorption in the infrared spectra of protein solutions in heavy water. *Biopolymers.* 14:679–694.

Fraser, R. D. B., and T. P. MacRae. 1973. Conformation in Fibrous Proteins and Related Synthetic Polypeptides. Academic Press, New York.

Frey, S., and L. K. Tamm. 1991. Orientation of melittin in phospholipid bilayers. A polarized attenuated total reflection infrared study. *Biophys. J.* 60:922–930.

Garten, W., F. X. Bosch, D. Linder, R. Rott, and H.-D. Klenk. 1981. Proteolytic activation of the influenza virus hemagglutinin: the structure of the cleavage site and the enzymes involved in cleavage. *Virology.* 115:361–374.

Gething, M. J., R. W. Doms, D. York, and J. White. 1986. Studies on the mechanism of membrane fusion: site-specific mutagenesis of the hemagglutinin of influenza virus. *J. Cell Biol.* 102:11–23.

Goormaghtigh, E., V. Cabiaux, and J.-M. Ruysschaert. 1994. Determination of soluble and membrane protein structure by Fourier transform infrared spectroscopy. III. Secondary structures. *In* Subcellular Biochemistry. H. J. Hilderson and G. B. Ralston, editors. Plenum Press, New York. 405–450.

Gordon, L. M., C. C. Curtain, Y. C. Zhong, A. Kirkpatrick, P. W. Mobley, and A. J. Waring. 1992. The amino-terminal peptide of HIV-1 glycoprotein 41 interacts with human erythrocyte membranes: peptide conformation, orientation and aggregation. *Biochim. Biophys. Acta.* 1139: 257–274.

Harter, C., P. James, T. Bächi, G. Semenza, and J. Brunner. 1989. Hydrophobic binding of the ectodomain of influenza hemagglutinin to membranes occurs through the "fusion peptide." *J. Biol. Chem.* 264: 6459–6464.

Ishiguro, R., N. Kimura, and S. Takahashi. 1993. Orientation of fusion-active synthetic peptides in phospholipid bilayers: determination by FTIR spectroscopy. *Biochemistry.* 32:9792–9797.

Krimm, S., and J. Bandekar. 1986. Vibrational spectroscopy and conformation of peptides, polypeptides, and proteins. *Adv. Protein Chem.* 38:181–364.

Lear, J. D., and W. F. DeGrado. 1987. Membrane binding and conformational properties of peptides representing the NH_2 terminus of inluenza HA-2. *J. Biol. Chem.* 262:6500–6505.

Levin, I. W., E. Mushayakarara, and R. Bittman. 1982. Vibrational assignment of the sn1 and sn2 carbonyl stretching modes of membrane phospholipids. *J. Raman Spectrosc.* 13:231–234.

Lewis, R. N. A. H., R. N. McElhaney, W. Pohle, and H. H. Mantsch. 1994. Components of the carbonyl stretching band in the infrared spectra of hydrated 1,2-diacylglycerolipid bilayers: a reevaluation. *Biophys. J.* 67: 2367–2375.

Lüneberg, J., I. Martin, F. Nüssler, J.-M. Ruysschaert, and A. Herrmann. 1995. Structure and topology of influenza virus fusion peptide in lipid bilayers. *J. Biol. Chem.* 270:27606–27614.

Mantsch, H. H., and R. N. McElhaney. 1991. Phospholipid phase transitions in model and biological membranes as studied by infrared spectroscopy. *Chem. Phys. Lipids.* 57:213–226.

Martin, I., F. Defrise-Quertin, E. Decroly, M. Vandenbranden, R. Brasseur, and J.-M. Ruysschaert. 1993. Orientation and structure of the NH_2-terminal HIV-1 gp41 peptide in fused and aggregated liposomes. *Biochim. Biophys. Acta.* 1145:124–133.

McIntosh, T. J., and Magid, A. D. 1993. Phospholipid hydration. *In* Phospholipids Handbook. G. Cevc, editor. Marcel Dekker, New York.

Mendelsohn, R., and H. H. Mantsch. 1986. Fourier transform infrared studies of lipid-protein interactions. *In* Progress in Protein-Lipid Interactions, Vol. 2. A. Watts and J. J. H. H. M. DePont, editors. Elsevier/ North Holland, Amsterdam.

Miyazawa, T., and E. R. Blout. 1961. The infrared spectra of polypeptides in various conformations: amide I and amide II bands. *J. Am. Chem. Soc.* 83:712–719.

Muga, A., W. Newgebauer, T. Hirama, and W. K. Surewicz. 1994. Membrane interaction and conformational properties of the putative fusion peptide of PH-30, a protein active in sperm-egg fusion. *Biochemistry.* 33:4444–4448.

Murata, M., Y. Sugahara, S. Takahashi, and S.-I. Ohnishi. 1987. pH-dependent membrane fusion activity of a synthetic 20 amino acid peptide with the same sequence as that of the hydrophobic segment of influenza virus hemagglutinin. *J. Biochem.* 102:957–962.

Murata, M., S. Takahashi, S. Kagiwada, A. Suzuki, and S.-I. Ohnishi. 1992. pH-dependent membrane fusion and vesiculation of phospholipid large unilamellar vesicles induced by amphiphilic anionic & cationic peptides. *Biochemistry.* 31:1986–1992.

Nieva, J. L., S. Nir, A. Muga, F. M. Goñi, and J. Wilschut. 1994. Interaction of the HIV-1 fusion peptide with phospholipid vesicles: different structural requirements for fusion and leakage. *Biochemistry.* 33:3201–3209.

Rafalski, M., J. D. Lear, and W. F. DeGrado. 1990. Phospholipid interactions of synthetic peptides representing the N-terminus of HIV gp41. *Biochemistry.* 29:7917–7922.

Rafalski, M., A. Ortiz, A. Rockwell, L. C. van Ginkel, J. D. Lear, W. F. DeGrado, and J. Wilschut. 1991. Membrane fusion acitivity of the influenza virus hemagglutinin: interaction of HA2 N-terminal peptides with phospholipid vesicles. *Biochemistry.* 30:10211–10220.

Rodionova, N. A., S. A. Tatulian, T. Surrey, F. Jähnig, and L. K. Tamm. 1995. Characterization of two membrane-bound forms of Omp A. *Biochemistry.* 34:1921–1929.

Ruigrok, R. W. H., A. Aitken, L. J. Calder, S. R. Martin, J. J. Skehel, S. A. Wharton, W. Weis, and D. C. Wiley. 1988. Studies on the structure of the influenza virus haemagglutinin at the pH of membrane fusion. *J. Gen. Virol.* 69:2785–2795.

Skehel, J. J., P. M. Bayley, E. B. Brown, S. R. Martin, M. D. Waterfield, J. M. White, I. A. Wilson, and D. C. Wiley. 1982. Changes in the conformation of influenza virus hemagglutinin at the pH optimum of virus-mediated membrane fusion. *Proc. Natl. Acad. Sci. USA.* 72:93–97.

Stegmann, T., F. P. Booy, and J. Wilschut. 1987. Effects of low pH on influenza virus. Activation and inactivation of the membrane fusion capacity of the hemagglutinin. *J. Biol. Chem.* 262:17744–17749.

Stegmann, T., J. M. Delfino, F. M. Richards, and A. Helenius. 1991. The HA2 subunit of influenza hemagglutinin inserts into target membrane prior to fusion. *J. Biol. Chem.* 266:18404–18410.

Steinhauer, D. A., S. A. Wharton, J. J. Skehel, and D. C. Wiley. 1995. Studies of the membrane fusion activities of fusion peptide mutants of influenza virus hemagglutinin. *J. Virol.* 69:6643–6651.

Surewicz, W. K., and H. H. Mantsch. 1988. New insight into protein secondary structure from resolution-enhanced IR spectra. *Biochim. Biophys. Acta.* 952:115–130.

Surewicz, W. K., H. H. Mantsch, and D. Chapman. 1993. Determination of protein secondary structure by Fourier transform infrared spectroscopy. *Biochemistry.* 32:7720–7726.

Tamm, L. K. 1988. Lateral diffusion and fluorescence microscope studies on a monoclonal antibody specifically bound to supported phospholipid bilayers. *Biochemistry.* 27:1450–1457.

Tamm, L. K., and S. A. Tatulian. 1993. Orientation of functional and nonfunctional PTS permease signal sequences in lipid bilayers. A polarized attenuated total reflection study. *Biochemistry.* 32:7720–7726.

Tatulian, S. A., P. Hinterdorfer, G. Baber, and L. K. Tamm. 1995a. Influenza hemagglutinin assumes a tilted conformation during membrane fusion as determined by attentuated total reflection FTIR spectroscopy. *EMBO J.* 14:5514–5523.

Tatulian, S. A., L. R. Jones, L. G. Reddy, D. L. Stokes, and L. K. Tamm. 1995b. Secondary structure and orientation of phospholamban reconstituted in supported bilayers from polarized attenuated total reflection FTIR spectroscopy. *Biochemistry.* 34:4448–4456.

Tsuboi, M. 1962. Infrared dichroism and molecular conformation of α-form poly-g-benzyl-L-glutamate. *J. Polym. Sci.* 59:139–153.

Tsurudome, M., R. Glück, R. Graf, R. Falchetto, U. Schaller, and J. Brunner. 1992. Lipid interactions of the hemagglutinin HA2 NH_2 segment during influenza virus-induced membrane fusion. *J. Biol. Chem.* 267:20225–20232.

Venyaminov, S. Y., and N. N. Kalnin. 1990. Quantitative IR spectrophotometry of peptide compounds in water (H_2O) solutions. I. Spectral parameters of amino acid residue absorption bands. *Biopolymers.* 30: 1243–1257.

Weber, T., G. Paesold, C. Galli, R. Mischler, G. Semenza, and J. Brunner. 1994. Evidence for H^+-induced insertion of influenza hemagglutinin HA2 N-terminal segment into viral membrane. *J. Biol. Chem.* 269: 18353–18358.

Wharton, S. A., L. J. Calder, R. W. H. Ruigrok, J. J. Skehel, D. J. Steinhauer, and D. C. Wiley. 1995. Electron microscopy of antibody complexes of influenza virus haemagglutinin in the fusion pH complex. *EMBO J.* 14:240–246.

Wharton, S. A., S. R. Martin, R. W. H. Ruigrok, J. J. Skehel, and D. C. Wiley. 1988. Membrane fusion by peptide analogues of influenza virus hemagglutinin. *J. Gen. Virol.* 69:1847–1857.

White, J. M. 1990. Viral and cellular membrane fusion proteins. *Annu. Rev. Physiol.* 52:675–697.

White, J. M. 1992b. Membrane fusion. *Science.* 258:917–924.

Wiley, D. C., and J. J. Skehel. 1987. The structure and function of the hemagglutinin membrane glycoprotein of influenza virus. *Annu. Rev. Biochem.* 56:365–394.

Wilson, I. A., J. J. Skehel, and D. C. Wiley. 1981. Structure of the haemagglutinin membrane glycoprotein of influenza virus at 3 Å resolution. *Nature.* 289:366–373.

Yang, J. T., C.-S. C. Wu, and H. M. Martinez. 1986. Calculation of protein conformation from circular dichroism. *Methods Enzymol.* 130:208–269.